Theor Chem Acc (1999) 103:64–69
DOI 10.1007/s002149900001

Theoretical
Chemistry Accounts

Letter

A theoretical study of the second band of the photoelectron spectrum of benzene with an analysis of the vibrational structure

Kouichi Takeshita

Faculty of Bioindustry, Tokyo University of Agriculture, Abashiri, Hokkaido 099-2422, Japan

Received: 20 August 1998 / Accepted: 15 January 1999 / Published online: 7 June 1999

Abstract. Ab initio calculations have been performed to study the second band of the photoelectron spectrum of benzene with analysis of the vibrational structure. The $^2E_{2g}$ and $^2A_{2u}$ states contribute to this band. In this study each contribution to the band is discussed. We propose that the onset of the band should be assigned to the 0-0 transition of the $^2A_{2u}$ state.

Key words: Franck–Condon factor – Theoretical intensity curve of ionization – ^2A_u and $^2E_{2g}$ of $C_6H_6^+$ – Normal vibrational calculation

1 Introduction

The electronic configuration of the ground state of benzene is represented by $\ldots 1a_{2u}{}^2 3e_{2g}{}^4 1e_{1g}^4$ with the D_{6h} symmetry point group. The $^2A_{2u}$ and $^2E_{2g}$ states contribute to the second band of the photoelectron spectrum (PES).

The second band has been observed in the energy range from 11.49 to 13 eV [1–4]. Several assignments of the spectrum have been reported. Considering the nature and magnitude of the effect of deuteration on the spectrum, Potts et al. [2] have proposed that the $^2A_{2u}$ and $^2E_{2g}$ states correspond to the lower-energy side and the higher-energy side, respectively.

Turner et al. [1] have reported the results of various molecular orbital calculations. All calculations gave the same result that the ionization potential of the $^2E_{2g}$ state was smaller than that of the $^2A_{2u}$ state. Kimura et al. [3] have reported the vertical ionization energy (VIE) obtained by ab initio calculations. The $^2E_{2g}$ and $^2A_{2u}$ states were assigned to the lower-energy side and the higher-energy side, respectively. As far as we are aware, all ab initio calculations [1, 3–5] give the VIE of the $^2E_{2g}$ state to be lower than that of the $^2A_{2u}$ state.

The band of the spectrum has two characteristics: one is the position of the band and the other is the shape. The position depends mainly on the electronic IE. The shape depends on the vibrational structure. It is, therefore, necessary to consider these two aspects for the assignment of the spectrum.

As the molecule is ionized, the equilibrium molecular structure is changed from that of the ground state. The VIE does not include this change. A zero–zero ionization energy (0-0 IE) gives the onset of the band. The 0-0 IE is determined by using the energy of the zero-point vibrational levels and the adiabatic ionization energy (AIE), which is the energy from the bottom to the bottom of the potential curve.

The shape of the band depends on the vibrational structure of the ionic state. The intensity of the vibrational excitation depends on the Franck–Condon factor (FCF), which is a function of the magnitude of the change in the equilibrium molecular structure and the vibrational wavefunction.

The $^2E_{2g}$ state is a doubly degenerate state. The molecular structure of the degenerate state should distort to one of lower symmetry such as D_{2h} symmetry by the Jahn–Teller distortion effect. The $^2E_{2g}$ state correlates to the ^2A_g and $^2B_{1g}$ states of D_{2h} symmetry. The molecular structure of the $^2E_{2g}$ state by the Jahn–Teller distortion within D_{2h} symmetry has been reported by Kato et al. [6].

The $^2A_{2u}$ state is not a degenerate state. The symmetry of the equilibrium molecular structure of the $^2A_{2u}$ state is the same D_{6h} symmetry as the ground state.

In this work, we study the equilibrium molecular structures of the $^2E_{2g}$ and $^2A_{2u}$ states by using the ab initio self-consistent-field (SCF) method. We calculated the ionization energies by means of single and double excitation configuration interaction (SDCI) calculations. We obtained the vibrational wavefunction using the normal vibrational calculation, the FCF, and the intensity curve.

Based on these calculations, we discuss an interpretation of the second band from the viewpoint of the position and shape of the band compared to the photoelectron spectrum.

2 Method of calculations

We used the basis sets of the MIDI-4-type prepared by Tatewaki and Huzinaga [7]. These are augmented by one p-type polarization function for H and one d-type polarization function for C. The exponents of the polarization functions for H and C are 0.68 and 0.61, respectively.

The gradient technique for Roothaan's restricted Hartree–Fock (RHF) method was employed to determine the optimum molecular structure of the ground state and of the ionic states.

The SDCI method was employed to obtain more accurate ionization energies for the estimation of the VIE and AIE. In the SDCI method, singly and doubly excited configuration state functions were generated where the inner shells were kept frozen. In the SDCI calculations, we used the D_{2h} symmetry point group.

The normal vibrational calculation of the totally symmetric modes was done by means of the gradient technique with the RHF wavefunction. We had some restrictions on the calculation of the FCFs: only the vibrational transitions to the totally symmetric modes of the ionic state were allowed and the initial state was the zero-point vibrational level of the ground state. The method of calculation of the FCFs and the theoretical intensity curves was the same as we used in a previous paper [8].

This work was carried out using the computer program system GRAMOL [9] for the gradient technique and the calculation of normal modes, and ALCHEMY II [10–12] was used for the CI calculations.

3 Results and discussion

The results of the optimized molecular structures of the ground and ionic states using the RHF method are listed in Table 1. The molecular structure of the D_{6h} symmetry of the $^2E_{2g}$ state distorts to the more stable structure of D_{2h} symmetry by the Jahn–Tellar effect. However, the nondegenerate $^2A_{2u}$ (D_{6h}) state of D_{6h} symmetry keeps the same symmetry. Table 1 also shows the magnitude of the change in the equilibrium molecular structure on ionization. For the $^2A_{2u}$ (D_{6h}) state, it shows that only the change in the C—C distance is recognizable. Kato et al. [6] have obtained optimized geometries for the ^2A_g (D_{2h}) and $^2B_{1g}$ (D_{2h}) states at the unrestricted HF/4-31 G level (Table 1).

3.1 Ionization energies

The VIE and AIE at the SCF level are given in Table 2. The VIE of the $^2A_{2u}$ (D_{6h}) state is larger than that of the $^2E_{2g}$ (D_{6h}) state, which is consistent with the calculations by Kimura et al. [3]. The AIE of the $^2A_{2u}$ (D_{6h}) state is also larger than those of the ^2A_g (D_{2h}) and $^2B_{1g}$ (D_{2h}) states.

The results of the SDCI calculations are given in Tables 3 and 4.

In the single-reference SDCI (SRSDCI) calculation, we used a reference configuration of the RHF wavefunction of the respective state and the D_{2h} symmetry point group. The configuration $\ldots 1a_{2u}^1 3e_{2g}^4 1e_{1g}^4$ of the $^2A_{2u}$ (D_{6h}) state correlates to the configuration $\ldots 1b_{1u}^1 6a_g^2 3b_{1g}^2 1b_{3g}^2 1b_{2g}^2$ of the $^2B_{1u}$ (D_{2h}) state. For the $^2A_{2u}$ (D_{6h}) state, Table 3 shows that the weight of the main configuration of $\ldots 1b_{1u}^1 6a_g^2 3b_{1g}^2 1b_{3g}^2 1b_{2g}^2$ is 81.9%. The weights of the reference configurations of the ^2A_g (D_{2h}) and $^2B_{1g}$ (D_{2h}) states are 82.8 and 82.3%, respectively. Table 4 shows that the VIE and AIE of the $^2A_{2u}$ (D_{6h}) state are larger than those of the ^2A_g (D_{2h}) and $^2B_{1g}$ (D_{2h}) states.

In the two-reference SDCI (2RSDCI) calculation, the weight of the configuration of the $^2A_{2u}$ (D_{6h}) state changes drastically compared to the SRSDCI calculation. The contribution of the main configuration decreases and that of the other configuration of $\ldots 1b_{1u}^2 6a_g^2 3b_{1g}^2 1b_{3g}^1 1b_{2g}^1 1a_u^1$ increases. The other configuration corresponds to the two-electron excitation of $1b_{3g}\,1b_{2g} \rightarrow 1b_{1u}\,1a_u$. For the ^2A_g (D_{2h}) and $^2B_{1g}$ (D_{2h}) states, we did not find any recognizable change in the weight of the main configuration. Table 4 shows that

Tabel 1. Optimized molecular structure and magnitude of the change in geometry upon ionization. Bond lengths are in angstroms, angles in degrees. The values in parentheses are the magnitudes of the change in geometry upon ionization. Kato et al. [6] have reported the following optimized geometries. For ^2A_g: C_1—C_2 = 1.355, C_2—C_3 = 1.441, C_1—H_1 = 1.108, C_2—H_2 = 1.072, C_2—C_1—C_6 = 127.5 and C_1—C_2—H_2 = 127.1. For $^2B_{1g}$: C_1—C_2 = 1.406, C_2—C_3 = 1.338, C_1—H_1 = 1.067, C_2—H_2 = 1.093, C_2—C_1—C_6 = 112.3 and C_1—C_2—H_2 = 113.1

State	C_1—C_2 (ΔC_1—C_2)	C_2—C_3 (ΔC_2—C_3)	C_1—H (ΔC_1—H)	C_2—H (ΔC_2—H)
^1A_g (D_{2h})	1.388	1.388	1.083	1.083
Exp.[a]	1.397	1.397	1.084	1.084
$^2A_{2u}$ (D_{6h})	1.420 (+0.032)	1.420 (+0.032)	1.081 (−0.002)	1.081 (−0.002)
^2A_g (D_{2h})	1.360 (−0.028)	1.440 (+0.052)	1.119 (+0.036)	1.084 (+0.001)
$^2B_{1g}$ (D_{2h})	1.407 (+0.019)	1.343 (−0.045)	1.077 (−0.006)	1.105 (+0.022)
State	C_6—C_1—C_2 (ΔC_6—C_1—C_2)	C_3—C_2—H (ΔC_3—C_2—H)		
^1A_g (D_{2h})	120.00	120.00		
Exp.[a]	120.00	120.00		
$^2A_{2u}$ (D_{6h})	120.00 (0.00)	120.00 (0.00)		
^2A_g (D_{2h})	127.77 (+7.77)	116.45 (−3.55)		
$^2B_{1g}$ (D_{2h})	112.32 (−7.68)	123.68 (+3.68)		

[a] Ref. [13]

Table 2. Veritcal ionization energies (*VIE*) and adiabatic ionization energies (*AIE*) from the restricted Hartree–Fock calculation. The total energy of ^1A_g is −230.442437 a.u.

State	VIE (eV)	AIE (eV)
$^2A_{2u}$ (D_{6h})	12.90	12.73
^2A_g (D_{2h})	12.69	12.15
$^2B_{1g}$ (D_{2h})	12.69	12.17

Table 3. Configuration interaction (*CI*) calculation of the $^2A_{2u}$ (D_{6h}) state using the D_{2h} symmetry point group. The configuration state functions (*CSF*) and the results of single-reference single and double excitation CI (*SRSDCI*) and two-reference SDCI (2*RSDCI*) calculations are listed

CSF	Weight of CSF (%)	
	SRSDCI	2RSDCI
$\ldots 1b_{1u}^1\ 6a_g^2\ 3b_{1g}^2\ 1b_{3g}^2\ 1b_{2g}^2$	81.9	63.5
$\ldots 1b_{1u}^2\ 6a_g^2\ 3b_{1g}^2\ 1b_{3g}^1\ 1b_{2g}^1\ 1a_u^1$	0.6	18.9

Table 4. Ionization energies (eV) from the SDCI calculations. Total energy of ^1A_g: −231.114102 (a.u.). The reference of the SRSDCI calculation of $^2A_{2u}$ (D_{6h}) is $\ldots 1b_{1u}^1\ 6a_g^2\ 3b_{1g}^2\ 1b_{3g}^2\ 1b_{2g}^2$ represented by the D_{2h} symmetry point group. The references of the SRSDCI calculation of ^2A_g (D_{2h}) and $^2B_{1g}$ (D_{2h}) are $\ldots 1b_{1u}^2\ 6a_g^1\ 3b_{1g}^2\ 1b_{3g}^2\ 1b_{2g}^2$ and $\ldots 1b_{1u}^2\ 6a_g^2\ 3b_{1g}^1\ 1b_{3g}^2\ 1b_{2g}^2$, respectively. For the 2RSDCI calculation of $^2A_{2u}$ (D_{6h}), the references are $\ldots 1b_{1u}^1\ 6a_g^2\ 3b_{1g}^2\ 1b_{3g}^2\ 1b_{2g}^2$ and $\ldots 1b_{1u}^2\ 6a_g^2\ 3b_{1g}^2\ 1b_{3g}^1\ 1b_{2g}^1\ 1a_u^1$

State	Method	VIE	AIE	0-0 IE	Franck–Condon factor
$^2A_{2u}$ (D_{6h})	SRSDCI	12.92	12.71		
	2RSDCI	12.04	11.78	11.77	0.289
^2A_g (D_{2h})	SRSDCI	12.40	11.92	11.89	0.043
$^2B_{1g}$ (D_{2h})	SRSDCI	12.40	11.92	11.91	0.040

the VIE and AIE of the $^2A_{2u}$ (D_{6h}) state are smaller than those of the ^2A_g (D_{2h}) and $^2B_{1g}$ (D_{2h}) states.

3.2 Normal vibrational calculation

The two a_{1g} and four e_{2g} vibrational modes of D_{6h} symmetry correlate to the a_g totally symmetric modes of D_{2h} symmetry. The vibrational frequencies of the six totally symmetric modes of the ^1A_g, ^2A_g and $^2B_{1g}$ states of D_{2h} symmetry are given in Table 5 along with the two a_{1g} vibrational modes of D_{6h} symmetry of the $^2A_{2u}$ state.

The observed vibrational frequencies of the ^1A_g state are given in Table 5. Comparing the calculated values and the observed values, we find that the calculated values are overestimated by 8.4–11.8%.

We characterize each mode by use of the conventional potential-energy distribution. Table 5 shows that the v_1 and v_2 modes are characterized as C—H stretching modes, the v_3 and v_5 modes are the C—C stretching modes, the v_4 mode is the C—C—H bending mode, and the v_6 mode is the C—C—C bending mode. The v_1 and v_5 modes correlate to the a_{1g} modes of D_{6h} symmetry.

3.3 Vibrational structure

We illustrated the theoretical intensity curve with a half width of 0.02 eV for each state. The theoretical intensity curves for the $^2A_{2u}$ (D_{6h}), ^2A_g (D_{2h}) and $^2B_{1g}$ (D_{2h}) states are illustrated in Figs. 1–3, respectively.

Figure 1 shows the vibrational structure of the $^2A_{2u}$ (D_{6h}) state: this has a very simple structure. An interpretation is given in Table 6. Only the v_5 mode is excited: this is the C—C stretching mode. This is connected to the change in the equilibrium molecular structure where only the change in the C—C distance is recognizable. The 0-0 transition has strong intensity. The 0-0 IE is 11.77 eV using the 2RSDCI calculation.

Figures 2 and 3 show the theoretical intensity curves of the ^2A_g (D_{2h}) and $^2B_{1g}$ (D_{2h}) states, respectively. An interpretation of each vibrational level is given in Tables 7 and 8. In both states, excitations of the v_3 and v_6 modes have considerable intensity. The v_3 and v_6 modes are the C—C stretching and C—C—C bending modes, respectively. This is connected to the change in the equilibrium molecular structure. Table 1 shows that there are distinguishable changes in the C—C bond length and in the C—C—C bond angle in both states. The 0-0 transitions had medium intensity, the magnitude of which was 15% of that of the $^2A_{2u}$ (D_{6h}) state. The 0-0 IEs of the ^2A_g (D_{2h}) and $^2B_{1g}$ (D_{2h}) states from the SRSDCI calculations are 11.89 and 11.91 eV, respectively.

3.4 Interpretation of the second band

The second band had an onset at 11.49 eV: this had a narrow peak and strong intensity. This peak was assigned to the 0-0 transition.

Using the result of the calculations of the 0-0 IE at the RHF or SRSDCI levels, we may assign the onset to the 0-0 transition of the ^2A_g (D_{2h}) and $^2B_{1g}$ (D_{2h}) states; however, the intensities of the 0-0 transitions of these states are so weak that we do not give a reasonable interpretation of the strong intensity of the first peak of the second band.

The results of the 2RSDCI calculations give a 0-0 IE for the $^2A_{2u}$ (D_{6h}) state 0.12–0.14 eV lower than for the ^2A_g (D_{2h}) and $^2B_{1g}$ (D_{2h}) states. The intensity of the 0-0 transition of the $^2A_{2u}$ (D_{6h}) state is 7 times stronger than that of the ^2A_g (D_{2h}) and $^2B_{1g}$ (D_{2h}) states. The overall feature of the intensity curve is shown in Fig. 4, and is compared with the observed PES of Turner et al. [1]. The vibrational structure of the theoretical intensity curve reproduces the PES well. This figure shows that the onset of the band is only due to the 0-0 transition of the $^2A_{2u}$ (D_{6h}) state. It also indicates that the ^2A_g (D_{2h}) and $^2B_{1g}$ (D_{2h}) states contribute to the higher vibrational levels above the second peak.

4 Conclusion

We studied the second band of the PES by ab initio calculations from the viewpoints of the position and the

Tabel 5. Vibrational frequencies (cm^{-1}) of the totally symmetric modes. The definitions of the symmetry coordinates are as follows: $\Delta S_1 = 1/2(\Delta C_1—C_2 + \Delta C_1—C_6 + \Delta C_3—C_4 + \Delta C_4—C_5)$, $\Delta S_2 = 1/\sqrt{2}(\Delta C_2—C_3 + \Delta C_5—C_6)$, $\Delta S_3 = 1/\sqrt{2}(\Delta C_1—H_1 + \Delta C_4—H_4)$, $\Delta S_4 = 1/2(\Delta C_2—H_2 + \Delta C_3—H_3 + \Delta C_5—H_5 + \Delta C_6—H_6)$, $\Delta S_5 = 1/\sqrt{2}(\Delta C_2—C_1—C_6 + \Delta C_3—C_4—C_5)$ and $\Delta S_6 = 1/2(\Delta C_3—C_2—H_2 + \Delta C_2—C_3—H_3 + \Delta C_6—C_5—H_5 + \Delta C_5—C_6—H_6)$, $\Delta S'_1 = 1/\sqrt{6}(\Delta C_1—C_2 + \Delta C_2—C_3 + \Delta C_3—C_4 + \Delta C_4—C_5 + \Delta C_5—C_6 + \Delta C_6—C_1)$ and $\Delta S'_2 = 1/\sqrt{6}(\Delta C_1—H_1 + \Delta C_2—H_2 + \Delta C_3—H_3 + \Delta C_4—H_4 + \Delta C_5—H_5 + \Delta C_6—H_6)$. The observed frequencies (Ref. [13]) of ν_1, ν_2, ν_3, ν_4, ν_5 and ν_6 are 3073, 3056, 1599, 1178, 995 and 608, respectively. The a_g modes of ν_1, ν_2, ν_3, ν_4, ν_5 and ν_6 (D_{2h} point group) correlate to the a_{1g}, e_{2g}, e_{2g}, e_{2g}, a_{1g} and e_{2g} modes (D_{6h} point group), respectively

State	Mode	Frequency	Conventional potential energy distribution (%)
^1A_g (D_{2h})	ν_1	3369	ΔS_4 (66), ΔS_3 (33)
	ν_2	3339	ΔS_3 (66), ΔS_4 (34)
	ν_3	1788	ΔS_2 (49), ΔS_1 (25), ΔS_6 (15), ΔS_5 (11)
	ν_4	1271	ΔS_6 (79), ΔS_2 (14), ΔS_1 (7)
	ν_5	1079	ΔS_1 (67), ΔS_2 (32)
	ν_6	660	ΔS_5 (77), ΔS_6 (20)
^2A_g (D_{2h})	ν_1	3358	ΔS_4 (99)
	ν_2	2961	ΔS_3 (98)
	ν_3	1602	ΔS_2 (36), ΔS_1 (32), ΔS_6 (18), ΔS_5 (12)
	ν_4	1224	ΔS_6 (73), ΔS_1 (20), ΔS_2 (7)
	ν_5	1048	ΔS_2 (52), ΔS_1 (43)
	ν_6	704	ΔS_5 (78), ΔS_6 (19)
$^2B_{1g}$ (D_{2h})	ν_1	3441	ΔS_3 (99)
	ν_2	3150	ΔS_4 (98)
	ν_3	1842	ΔS_2 (62), ΔS_1 (22), ΔS_5 (8)
	ν_4	1164	ΔS_6 (90), ΔS_2 (9),
	ν_5	1057	ΔS_1 (76), ΔS_2 (22)
	ν_6	602	ΔS_5 (73), ΔS_6 (24)
$^2A_{2u}$ (D_{6h})	ν_1	3408	$\Delta S'_2$ (99)
	ν_5	1026	$\Delta S'_1$ (99)

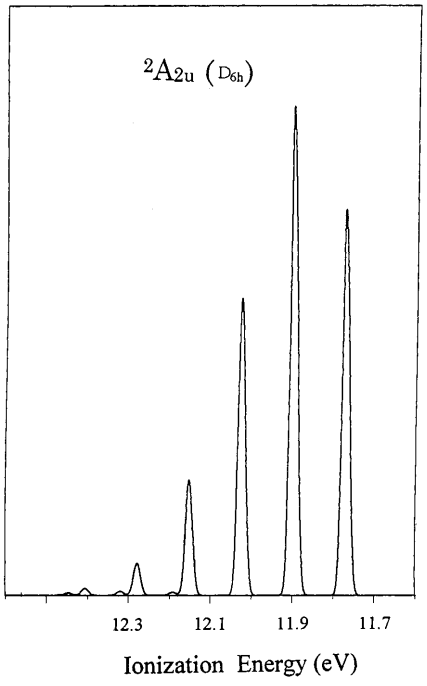

Fig. 1. The theoretical intensity curves (*TICs*) of the ionization energy of the $^2A_{2u}$ (D_{6h}) state with a half width of 0.02 eV

shape of the band. The $^2E_{2g}$ (D_{6h}) state distorts to the ^2A_g and $^2B_{1g}$ states of D_{2h} symmetry. The $^2A_{2u}$ (D_{6h}), ^2A_g (D_{2h}) and $^2B_{1g}$ (D_{2h}) states contribute to the second band.

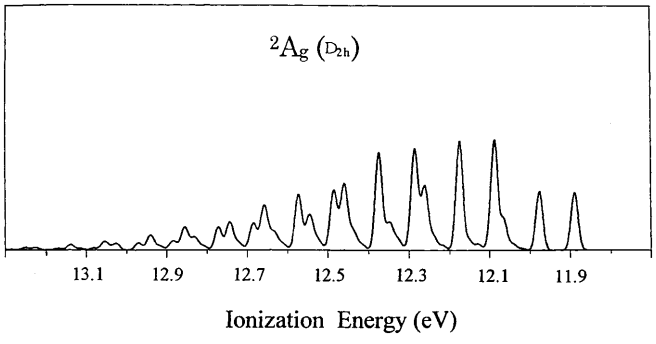

Fig. 2. The TICs of the ionization energy of the ^2A_g (D_{2h}) state with a half width of 0.02 eV

The onset of the second band of the PES has a strong intensity. The FCF calculations reveals that the intensity of the 0-0 transition of the $^2A_{2u}$ (D_{6h}) state is 7 times stronger than that of the ^2A_g (D_{2h}) and $^2B_{1g}$ (D_{2h}) states. Therefore, the onset of the PES should be connected to the 0-0 transition of the $^2A_{2u}$ (D_{6h}) state.

The 0-0 IEs of the ^2A_g (D_{2h}) and $^2B_{1g}$ (D_{2h}) states at the RHF or SRSDCI levels are lower than that of $^2A_{2u}$ (D_{6h}) state by 0.8 eV; therefore, the calculations at the RHF or SRSDCI levels do not give a reasonable 0-0 IE for the assignment of the onset of the second band.

The 2RSDCI calculations gives the 0-0 IE of the $^2A_{2u}$ (D_{6h}) state to be 0.12–0.14 eV lower than those of the ^2A_g (D_{2h}) and $^2B_{1g}$ (D_{2h}) states. Using this result, we obtained a reasonable theoretical intensity curve compared with the second band of the PES. Therefore, we

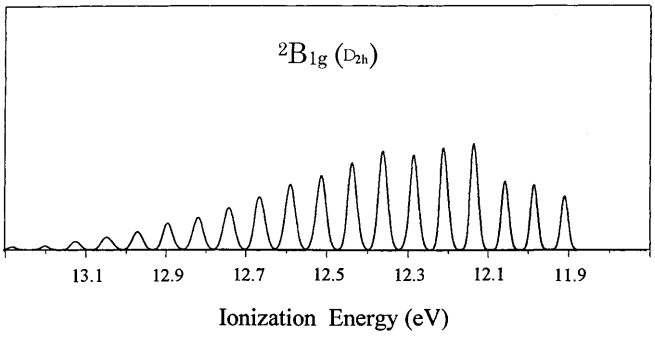

Fig. 3. The TICs of the ionization energy of the $^2B_{1g}$ (D_{2h}) state with a half width of 0.02 eV

Table 6. Vibrational levels of the $^2A_{2u}$ (D_{6h}) state. The intensity is classified into s or m according to the magnitude of the Franck–Condon factors (*FCF*) as follows. s: 0.06 < FCF < 0.37 and m: 0.03 < FCF < 0.06

IE	Vibrational levels
11.77	s (0 0)
11.90	s (0 1)
12.02	s (0 2)
12.15	s (0 3)
12.28	m (0 4)

Table 7. Vibrational levels of the ^2A_g (D_{2h}) state. The intensity is classified into s, m or w according to the magnitude of the FCFs as follows s: 0.08 < FCF < 0.09, m: 0.03 < FCF < 0.05 and w: 0.01 < FCF < 0.03

IE	Vibrational levels
11.89	0 (m)
11.98	v_6 (m)
12.60–12.09	$2v_6$ (w), v_3 (s)
12.18	$v_3 + v_6$ (s)
12.26–12.29	$v_3 + 2v_6$ (m), $2v_3$ (s)
12.35–12.38	$v_3 + 3v_6$ (w), $2v_3 + v_6$ (s)
12.46–12.49	$v_2 + v_3$ (w), $2v_3 + 2v_6$ (m), $3v_3$ (m)
12.54–12.57	$v_2 + v_3 + v_6$ (w), $2v_3 + 3v_6$ (w), $3v_3 + v_6$ (m)
12.65–12.68	$4v_3$ (w), $v_2 + 2v_3$ (w), $3v_3 + 2v_6$ (w)
12.74–12.77	$4v_3 + v_6$ (w), $v_2 + 2v_3 + v_6$ (w)
12.85	$v_2 + 3v_3$ (w)

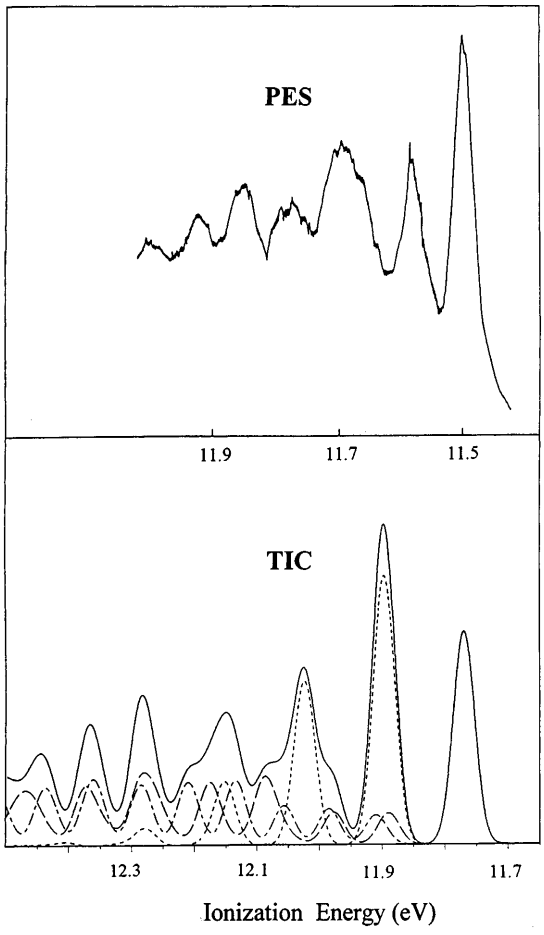

Fig. 4. The TICs of the ionization energy of the second band with a half width of 0.04 eV and the observed photoelectron spectrum (*PES*) of Turner et al. [1]. Each *line* illustrates the TIC as follows: *solid line*: the total intensity curve: *dotted line*: $^2A_{2u}$ (D_{6h}); *dashed line*: ^2A_g (D_{2h}); *dashed dotted line*: $^2B_{1g}$ (D_{2h})

propose that the onset of the band at 11.49 eV is the 0-0 transition of the $^2A_{2u}$ (D_{6h}) state and the ^2A_g (D_{2h}) and $^2B_{1g}$ (D_{2h}) states contribute to the intensity of the higher-energy region.

In the 2RSDCI calculation of the $^2A_{2u}$ (D_{6h}) state, the contribution of the double excitation of $1b_{3g}\,1b_{2g} \rightarrow 1b_{1u}\,1a_u$ (D_{2h}) increases.

Table 8. Vibrational levels of the $^2B_{1g}$ (D_{2h}) state. The intensity is classified into m or w according to the magnitude of the FCFs as follows m: 0.03 < FCF < 0.06 and w: 0.01 < FCF < 0.03

IE	Vibrational levels
11.91	0 (m)
11.98	v_6 (m)
12.05–12.06	$2v_6$ (w), v_4 (w)
12.13–12.14	$3v_6$ (w), $v_4 + v_6$ (m), v_3 (m)
12.20–12.21	$v_4 + 2v_6$ (w), $v_3 + v_6$ (m)
12.28–12.29	$v_3 + 2v_6$ (m), $v_3 + v_4$ (w)
12.36–12.37	$v_3 + 3v_6$ (w), $v_3 + v_4 + v_6$ (m), $2v_3$ (w)
12.43–12.44	$2v_3 + v_6$ (m), $v_3 + v_4 + 2v_6$ (w)
12.50–12.52	$2v_3 + 2v_6$ (w), $v_3 + 2v_4 + v_6$ (w)
	$2v_3 + v_4$ (w)
12.59–12.60	$3v_3$ (w), $2v_3 + v_4 + v_6$ (w), $v_2 + v_3 + v_6$ (w)
12.66–12.67	$3v_3 + v_6$ (w), $2v_3 + v_4 + 2v_6$ (w)

Acknowledgement. The computations were carried out on HITAC M-680H systems at the Center for Information Processing Education of Hokkaido University.

References

1. Turner DW, Baker AD, Baker C, Brundel CR (1970) Molecular photoelectron spectroscopy. Wiley-Interscience, London
2. Potts AW, Price WC, Streets DG, Williams TA (1972) Faraday Discuss Chem Soc 54: 168
3. Kimura K, Katsumata S, Achiba Y, Yamazaki T, Iwata S (1981) Handbook of HeI photoelectron spectra of fundamental organic molecules. Halsted, New York
4. Baltzer P, Karlsson L, Wannberg B, Öhrwall G, Holland DMP, MacDonald MA, Hayes MA, von Niessen W (1997) Chem Phys 224: 95
5. Masuda S, Aoyama M, Ohno K, Harada Y (1990) Phys Rev Lett 65: 3257
6. Kato H, Hirao K, Sano M (1983) J Mol Struct 104: 489
7. Tatewaki H, Huzinaga S (1980) J Comput Chem 1: 205
8. Takeshita K (1987) J Chem Phys 86: 329
9. Takeshita K, Sasaki F (1981) Library program at the Hokkaido University Computing Center (in Japanese). GRAMOL included the Program JAMOL3 of the RHF calculation written by Kashiwagi H, Takada T, Miyoshi E, Obara S for the Library program at the Hokkaido University Computing Center (in Japanese)
10. Lengsfield BH III (1980) J Chem Phys 73: 382
11. Liu B, Yosimine M (1981) J Chem Phys 74: 612
12. Lengsfield BH III, Liu B (1981) J Chem Phys 75: 478
13. Herzberg G (1966) Molecular spectra and molecular structure, part III. Van Nostrand, New York